A Comparison of Numerical Solutions of the Boltzmann Transport Equation for High-Energy Electron Transport Silicon

Antonio Abramo, L. Baudry, Rosella Brunetti, Rene Castagne, M. Charef, F. Dessenne, Philippe Dollfus, Robert Dutton, W. L. Engl, R. Fauquembergue, Claudio Fiegna, Massimo V. Fischetti, Sylvie Galdin, Neil Goldsman, Michael Hackel, Chihiro Hamaguchi, Karl Hess, Ken Hennacy, Patrice Hesto, Jack M. Higman, Takahiro Iizuka, C. Jungemann, Y. Kamakura, Hans Kosina, T. Kunikiyo, Steven E. Laux, Hongchin Lin, Christine Maziar, Hiroyuki Mizuno, H. J. Peifer, Sridhar Ramaswamy, Nobuyuki Sano, Paul G. Scrobohaci, Siegfried Selberherr, M. Takenaka, Ting-wei Tang, Kenji Taniguchi, J. L. Thobel, R. Thoma, Kazutaka Tomizawa, Masaaki Tomizawa, Thomas Vogelsang, Shiuh-Luen Wang, Xiaolin Wang, Chiang-Sheng Yao, P. D. Yoder, and Akira Yoshii

Abstract—**In this work we have undertaken a comparison of several previously reported computer codes which solve the semi-classical Boltzmann equation for electron transport in silicon. Most of the codes are based on the Monte Carlo particle technique, and have been used here to calculate a relatively simple set of transport characteristics, such as the average electron energy. The results have been contributed by researchers from Japan, Europe, and the United States, and the results were subsequently collected by an independent observer. Although the computed data vary widely, depending on the models and input parameters which are used, they provide for the first time a quantitative (though not comprehensive) comparison of Boltzmann Equation solutions.**

Manuscript received December 17, 1993; revised May 16, 1994. The review of this paper was arranged by Associate Editor D. A. Antoniadis. This work was supported by the National Science Foundation through the National Center for Computational Electronics at the University of Illinois, Urbana-Champaign.

A. Abramo and C. Fiegna are with DEIS, University of Bologna, 40137 Bologna, Italy.

L. Baudry, M. Charef, F. Dessenne, R. Fauquembergue, and J. L. Thobel are with IEMN (UA CNRS 9929), Departement Hyperfrequences et Semiconducteurs, Universite des Sciences et Technologies de Lille, Cite Scientifique Bt P3, 59655 Villeneuve d'Ascq, France.

R. Brunetti is with the University of Modena, Modena, Italy.

R. Castagne, P. Dollfus, S. Galdin, and P. Hesto are with the Institut d'Electronique Fondamentale, CNRS URA22, Universite Paris-Sud, Bat. 220, 91405 Orsay Cedex, France.

R. Dutton and C.-S. Yao are with the Integrated Circuits Laboratory, Stanford University, Stanford, CA 94305 USA.

W. L. Engl, C. Jungemann, H. J. Peifer, and R. Thoma are with the Institut für Theoretische Elektrotechnik, University of Aachen, 52056 Aachen, Germany.

M. Fischetti and S. E. Laux are with IBM Research Division, Thomas J. Watson Research Center, Yorktown Heights, NY 10598 USA.

N. Goldsman, K. Hennacy, H. Lin, and S.-L. Wang are with the Department of Electrical Engineering, University of Maryland, College Park, MD 20742 USA.

M. Hackel, H. Kosina, and S. Selberherr are with the Institute for Microelectronics, Technical University of Vienna, A-1040 Vienna, Austria.

C. Hamaguchi, Y. Kamakura, H. Mizuno, and K. Taniguchi are with the Department of Electronic Engineering, Osaka University, Suita, Osaka 565, Japan.

K. Hess, J. M. Higman, and P. D. Yoder are with the Beckman Institute, University of Illinois at Urbana-Champaign, Urbana, IL 61801 USA.

T. Iizuka is with the Microelectronics Research Laboratories, NEC Corp., 1120 Shimokuzawa, Sagamihara, Kanagawa 229, Japan.

T. Kunikiyo is with the LSI Laboratory, Mitsubishi Electric Corporation, Mizuhara, Itami 664, Japan.

C. Maziar and X. Wang are with the Microelectronics Research Center, The University of Texas at Austin, TX 78712 USA.

S. Ramaswamy, P. G. Scrobohaci, and T.-W. Tang are with the Department of Electrical Engineering, University of Massachusetts, Amherst, MA 01003 USA.

N. Sano, M. Tomizawa, and A. Yoshii are with NTT LSI Laboratories, 3-1 Morinosato Wakamiya, Atsugi-shi, Kanagawa 243-01, Japan.

M. Tanenaka is with VLSI Research Laboratory, Sharp Corporation, Ichinomoto Tenri, Nara 632, Japan.

K. Tomizawa is with the Department of Computer Science, Meiji University, 1-1-1 Higashimita, Tama-ku, Kawasaki, Japan.

T. Vogelsang is with Siemens AG, Central Research and Development BT ACM, München, Germany.

IEEE Log Number 9403543.

I. Introduction

As the available computing power increases, it has become more appealing to solve the Boltzmann Transport equation for electronic transport in semiconductors, as opposed to solving approximate sets of equations based on moments of the Boltzmann equation. Solutions of the Boltzmann equation allow one to investigate particular transport phenomena on a microscopic scale, and under the best of circumstances to simulate realistic devices. While solutions of the Boltzmann equation can be replaced by simpler models and methods for limited energy ranges, effects such as impact ionization, that require the knowledge of the electron distribution over an energy range of several electron volts, demand a more fundamental approach. The availability of computational resources has often forced researchers to make approximations beyond those inherent in the Boltzmann equation itself, and each of the existing transport simulation codes is a highly individualized collection of physical approximations and numerical algorithms. The choice of models and algorithms is often dictated by the particular phenomena and energy range of interest. It is nearly impossible to compare the simulations in detail, since most of them exist in either university or industrial laboratories and are not available in the public domain. The National Center for Computational Electronics (NCCE) has provided an organization within which a direct comparison

0018-9383/94$04.00 © 1994 IEEE

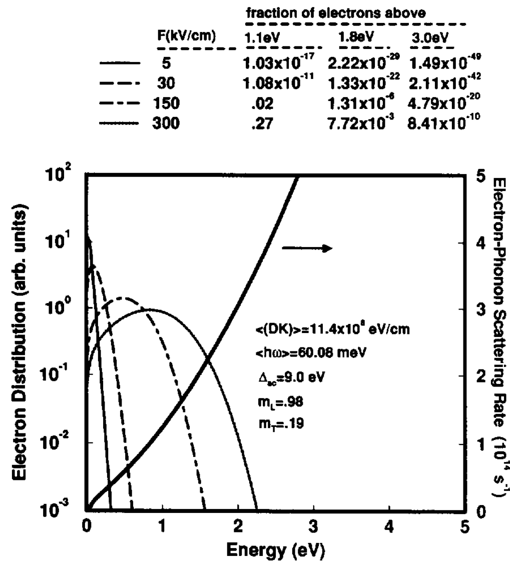

Fig. 1. The first three Legendre polynomials are used [15], [25]. (Goldsman, Hennacy, Lin, S.-L. Wang).

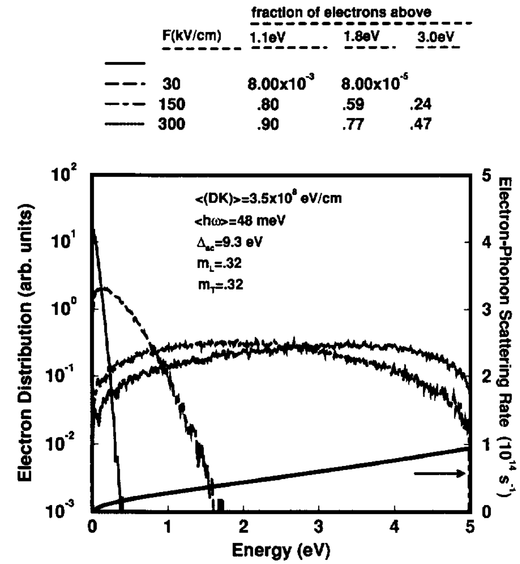

Fig. 2. Parbolic, spherical bandmodel, six equivalent valleys [18], [19]. (Hesto, Galdin, Dolfus, Castagne).

has been performed [1], and this paper documents our results. We emphasize that this study is not meant to be the final word on transport simulation, but rather a starting point for an open discussion.

We have focused this study on a single issue, the physical models and their consequences for the high energy tail of the electron distribution, which controls, for example, impact ionization and electron injection from silicon into its oxide. The calculations deal with transport at electric field strengths typical of those found in modern MOS transistors, and represent the kind of calculation that we would like to be able to do with confidence.

The results should be of use to those interested in constructing a transport (or device) simulation program, in that one can see various approximations to the Boltzmann Transport Equation applied to the same example problem. This work thus serves as a companion to each of the previous publications regarding the models. Furthermore, these results represent a benchmark for the state-of-the-art in semiclassical transport simulation.

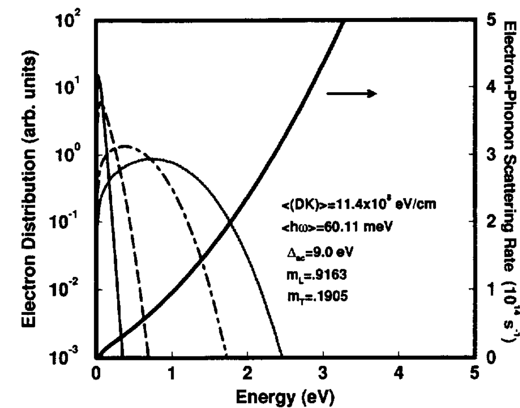

Fig. 3. Nonparabolic, ellipsoidal band model [15], [17]. (Kosina, Hackel, Selberherr).

II. The Calculation

Each simulation code was used to calculate the energy distribution of electrons in homogeneous, intrinsic silicon at room temperature with time-invariant applied electric fields of 5 kV/cm, 30 kV/cm, 150 kV/cm, and 300 kV/cm. For each field, the percentage of electrons above 1.1 eV, 1.8 eV, and 3.1 eV were calculated. For intrinsic silicon the effects of electron-electron scattering and impurity scattering need not be included in the simulation.

Figs. 1–20 show these data for each model, along with the effective scattering parameters, and electron-phonon scattering rates. The data sets have been arranged in order of increasing complexity of bandstructure models, i.e., Figs. 1–7 use effective mass bandstructures (only Fig. 2 uses parabolic bands, all others are nonparabolic). The model corresponding to Fig. 8 uses effective mass bands, including nonparabolic, ellipsoidal bands at the band minimum, and spherical parabolic bands for higher lying minima. Figs. 9–16 represent the fit-band models (discussed also in the Appendix) which use analytic functions with adjustable parameters to capture some features of the full bandstructure while maintaining the advantages of analytic energy momentum relationships.

Figs. 17–21 represent the full band models, where the bandstructure is calculated using a pseudopotential approach

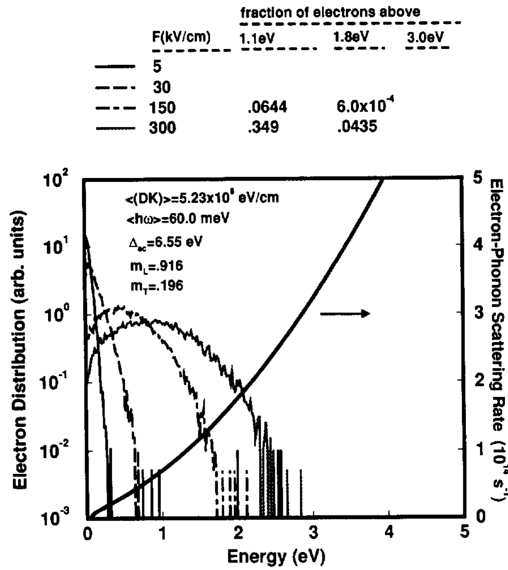

Fig. 4. Nonparabolic, ellipsoidal band model [40]. (K. Tomizawa).

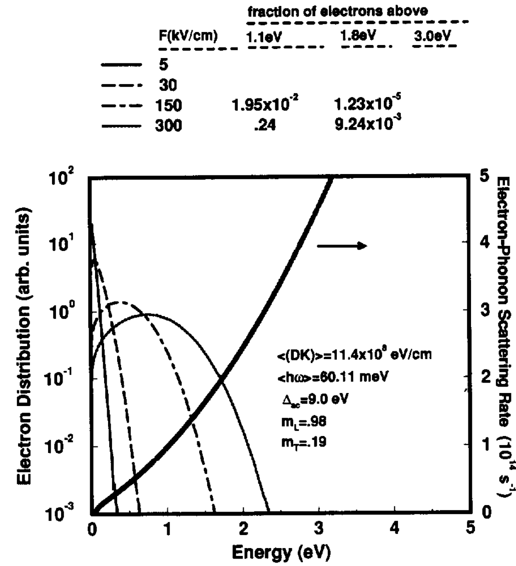

Fig. 6. Nonparabolic, ellipsoidal band model [5]. (Ramaswamy, Tang).

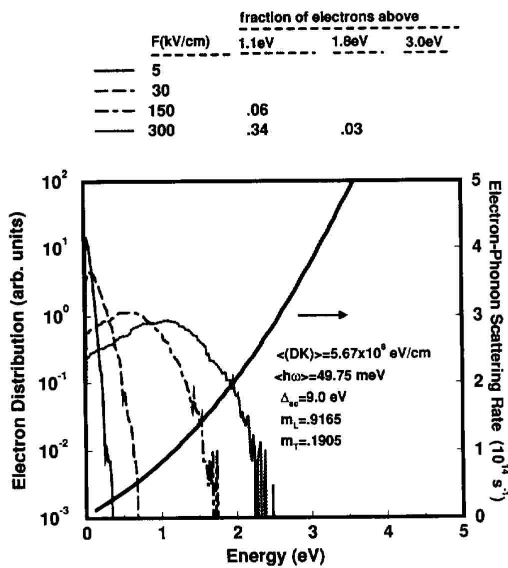

Fig. 5. Nonparabolic, ellipsoidal band model [27], [28]. (Charef, Dessenne, Thobel, Baudry, Fauquembergue).

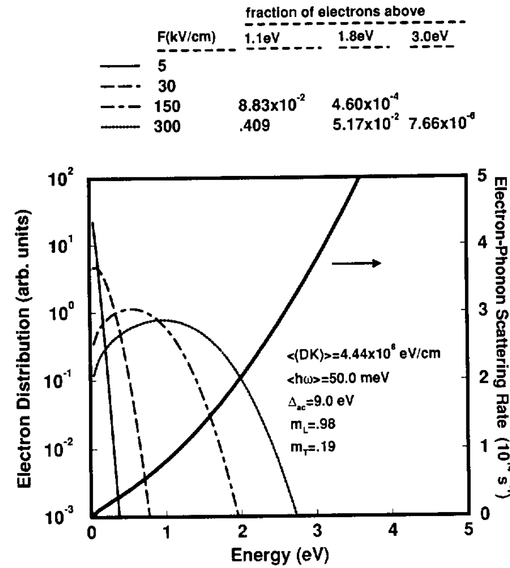

Fig. 7. Nonparabolic, ellipsoidal band model [7], [8]. (Iizuka).

(see [14] for a summary of relevant pseudopotential parameters), and tabulated on a 3-D grid in momentum space. The latter three data sets, shown in Figs. 19–21, use not only full pseudopotential bandstructures, but also electron-phonon matrix elements (coupling) calculated from the pseudopotential description of the crystal, as opposed to using phenomenological coupling constants as in models 1–18.

We have chosen to simply plot the total electron-phonon scattering (emission plus absorption) rates as a function of energy for each model. Although this is an incomplete representation of any particular transport model (the relative magnitudes of rates for different mechanisms and the impact ionization rate are not shown) it does give some indication about the density of electronic states and the strength of the electron-phonon coupling which was used in the model. At high electric fields the impact ionization scattering rate will also have a strong effect on the calculated electron distribution and the details of the ionization scattering rates can be found in the references given for each data set. Recent work on the impact ionization in silicon [22], [41], [42] has furthered our understanding of the underlying physics as well as our ability to construct physically realistic ionization scattering rates. The Appendix contains a derivation of the electron-phonon scattering rates, an explanation of the various approximations which are typically used, and a definition of the parameters

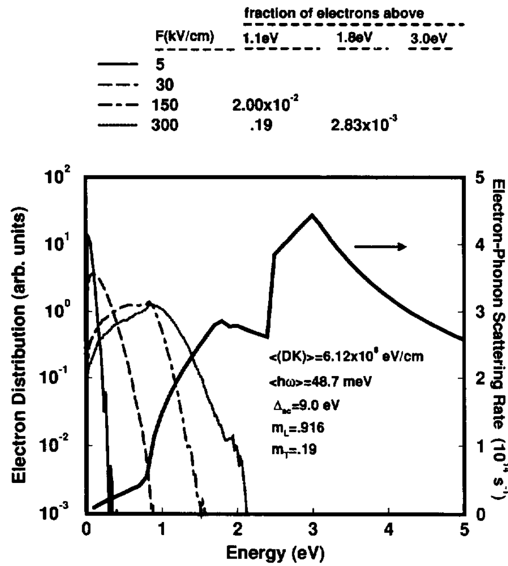

Fig. 8. Nonparabolic, ellipsoidal band model for X-valleys, parabolic, spherical band model for L-valleys [21], [22]. (Sano, M. Tomizawa, Yoshii).

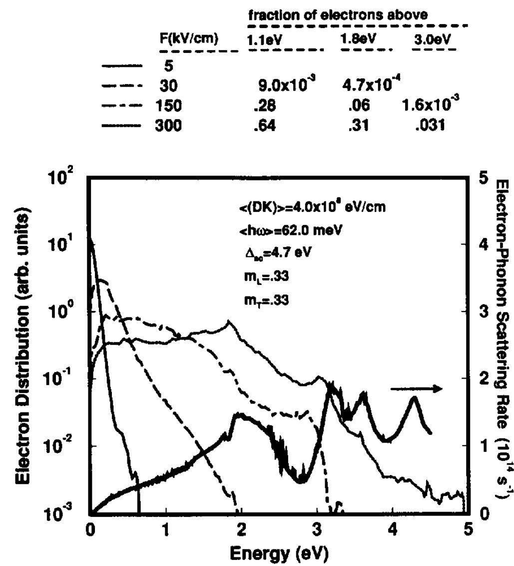

Fig. 10. Analytic fit band model [2] (Vogelsang).

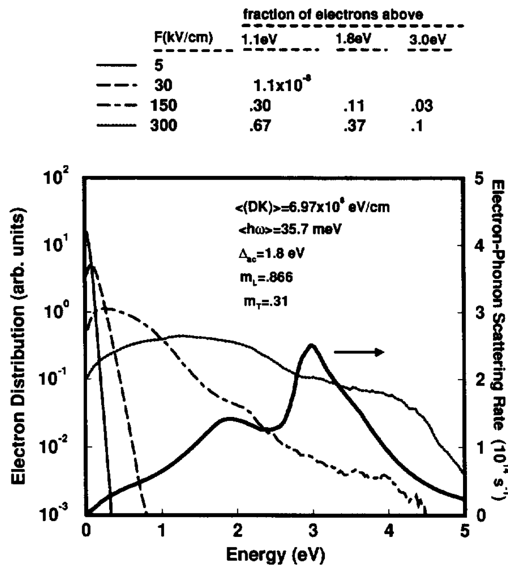

Fig. 9. Analytic fit band model [4], [24]: (Wang, Maziar).

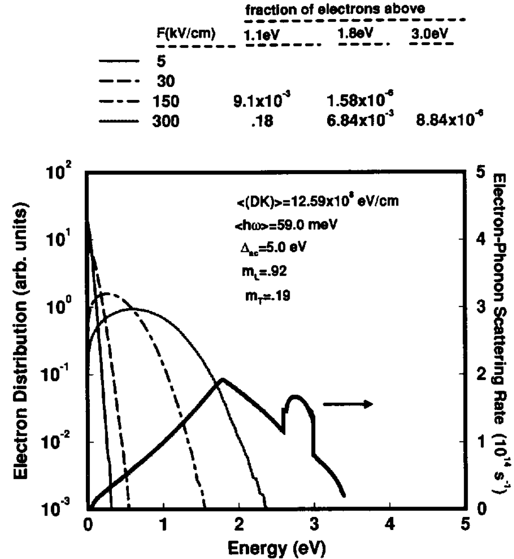

Fig. 11. Analytic fit band model [4] (Scrobohaci, Tang).

which are listed in the figures. The figure captions indicate the type of bandstructure model used, references which describe the models, and the names of the individual contributors.

Fig. 22 shows a collective plot of the data for the average energy of the electron distribution as a function of the applied field. This figure summarizes a certain lack of consensus, as we observe that the average energy can span nearly one order of magnitude from the highest to lowest result, even for fields as low as 30 kV/cm. We emphasize, however, that the various models have been developed for certain purposes and to be used in specific energy ranges. The models may give "correct" results for the energy range for which they have been constructed but fail to agree for the average energy.

In summary, we can say that there is significant, often *vast*, difference even between models which would at first appear to be similar. This result indicates that our collective understanding of, and ability to simulate, electronic transport in silicon calls for a more unified approach and for a clear understanding of one's goals before a simplified model is used.

Appendix A
Summary of Electron-Phonon Scattering Models and Band Models in Silicon

Here we summarize the formulas for the nonpolar electron-phonon scattering rates typically used in semiclassical Monte Carlo simulations of electronic transport in silicon. As general references we refer the reader to the books by Conwell [31]

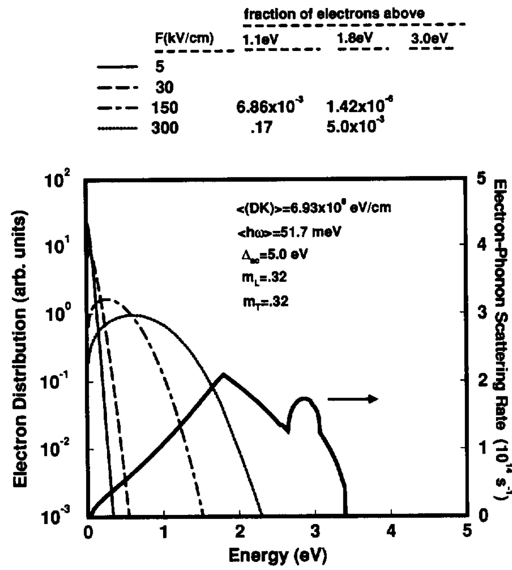

Fig. 12. Analytic fit band model [4], [9], [10]. (Peifer, Thoma, Jungemann, Engl).

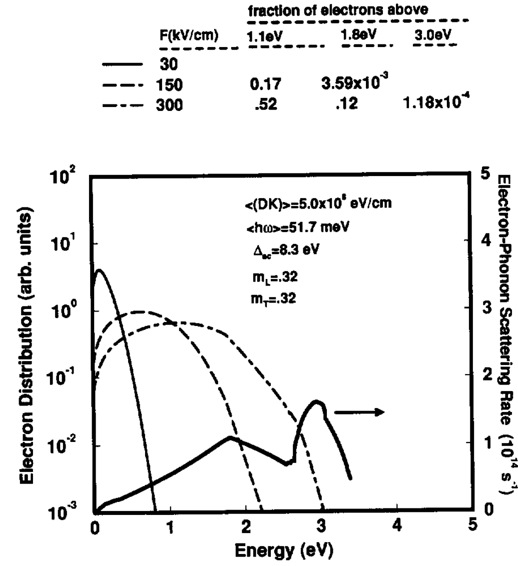

Fig. 14. Analytic fit band model [4], [11], [12]. (Fiegna).

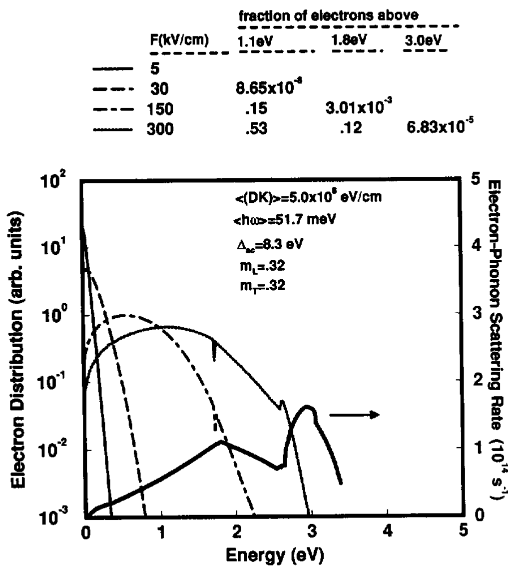

Fig. 13. Analytic fit band model [4],]11]. (Fiegna, Brunetti).

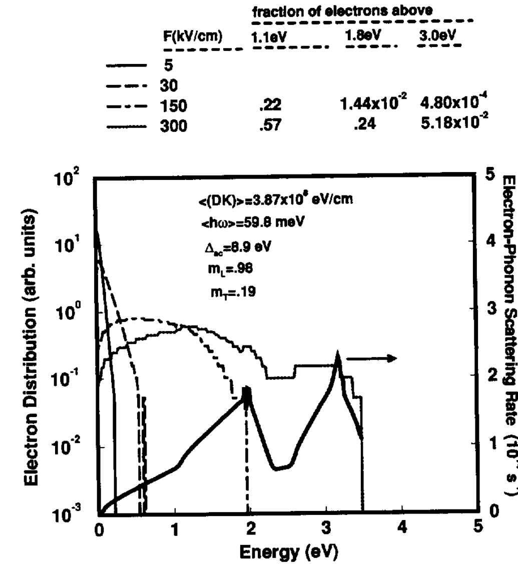

Fig. 15. Analytic fit band model [20]. (Mizuno, Taniguchi, Hamaguchi).

and Ridley [32], and the work of Seitz [33] and Harrison [34], which although not strictly applicable to intervalley scattering in silicon, have nonetheless formed the theoretical basis for most of the models which are currently in use. The coupling to the long wavelength acoustic phonons (intravalley scattering) via the deformation potential interaction was given by Shockley and Bardeen [35]. In this Appendix we attempt to review the subject with sufficient generality to explain the scattering rates used in virtually all of the silicon transport simulations in use today [36].

One usually starts with Fermi's Golden rule, (see, for example, [37]) for the quantum mechanical probabilities per unit time of scattering from a state $|\mathbf{k}>$ to $|\mathbf{k}'>$ (the vectors $\mathbf{k}$ are wavevectors in the first Brillouin zone, and the states labeled by these wavevectors are Bloch states)

$$\frac{1}{\tau(\mathbf{k})} = \frac{2\pi}{\hbar} \sum_{\eta,\mathbf{k}'} |M_\eta(\mathbf{k},\mathbf{k}')|^2 \delta(E(\mathbf{k}') - E(\mathbf{k}) \pm \hbar\omega_{\mathbf{q},\eta}) \times (N_{\mathbf{q},\eta} + 1/2 \pm 1/2). \quad \text{(A1)}$$

This is the rate at which electrons scatter out of state $|\mathbf{k}>$ to all possible final states $|\mathbf{k}'>$ $\hbar$ is the reduced Planck constant, the upper signs are for emission and the lower signs are for absorption, $\hbar\omega_{\mathbf{q},\eta}$ is the energy of the phonon of branch η, with wavevector $\mathbf{q}$. $M_\eta(\mathbf{k},\mathbf{k}') = \langle \mathbf{k}|H_{e-\mathrm{ph}}|\mathbf{k}'\rangle$ is the

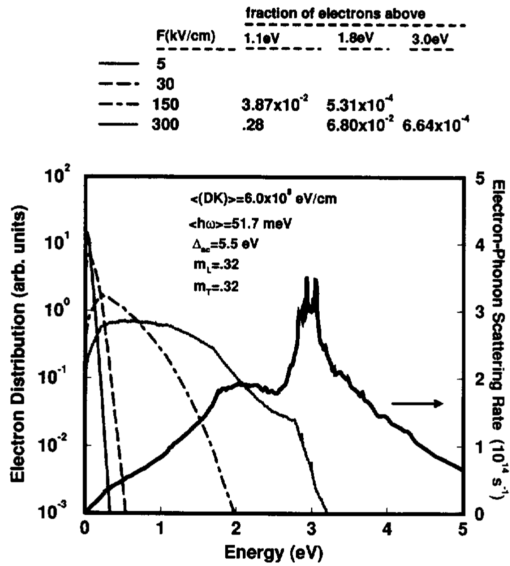

Fig. 16. Analytic fit band model [29], [30]. (Abramo, Yao).

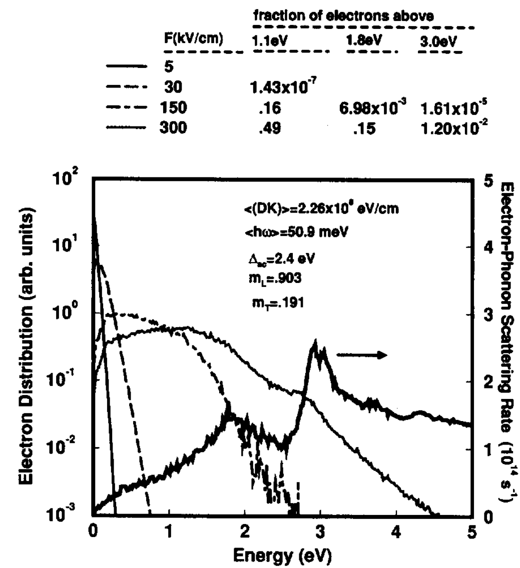

Fig. 18. Full band model [13], [14]. (Fischetti, Laux).

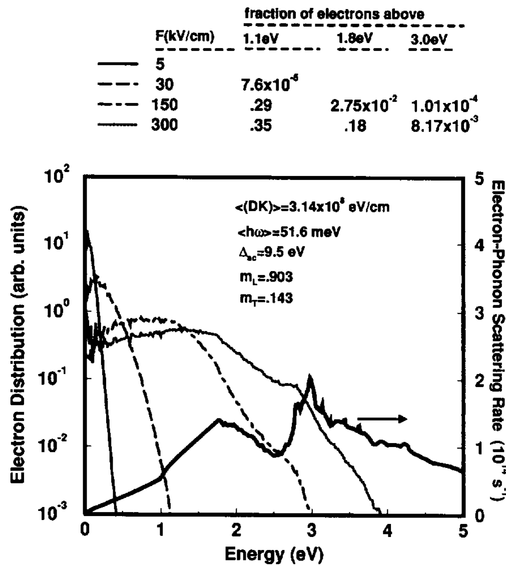

Fig. 17. Full band model [3], [36], [41]. (Higman, Hess).

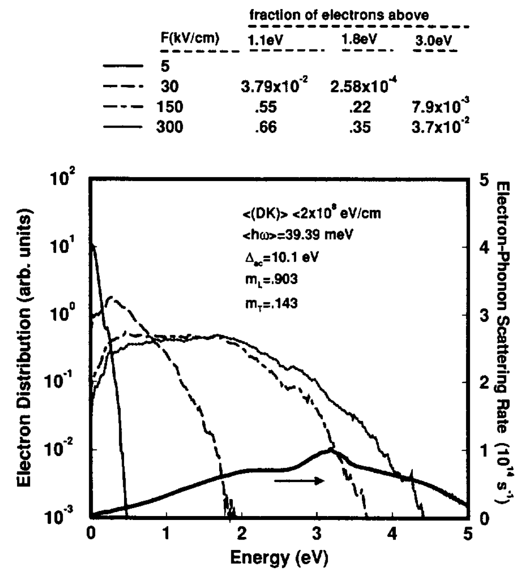

Fig. 19. Full band model [6]; no adjustable electron-phonon parameters in this model. (Yoder, Higman, Hess).

matrix element of the perturbing electron-phonon interaction potential. $N_{\mathbf{q},\eta}$ is the average phonon occupation given by the Bose–Einstein distribution. Crystal momentum is conserved through the additional relation $\mathbf{q} = \mathbf{k} - \mathbf{k}' + \mathbf{G}_u$, where $\mathbf{q}$ is the phonon wavevector confined to the first Brillouin zone, and $\mathbf{G}_u$ is a reciprocal lattice vector which is by definition zero for Normal processes and nonzero for Umklapp processes. In the case of scattering between any of the six equivalent conduction band minima in silicon, $\mathbf{G}_u$ is nonzero. In order to simplify the notation we assume a single conduction band, and the many band derivation would require only additional band labels on the electronic states. In the final result (A7) we indicate how one generalizes to a many-band model.

The general electron-phonon coupling strength is defined as

$$\Delta_\eta(\mathbf{k}, \mathbf{k}') = \left[\frac{2\rho V \omega_{\mathbf{q},\eta}}{\hbar}\right]^{\frac{1}{2}} |M_\eta(\mathbf{k}, \mathbf{k}')| \qquad \text{(A2)}$$

where ρ is the mass density of the crystal and V is the macroscopic volume of the crystal. The scattering models which are in common use may be obtained by making the critical assumption that the coupling strength Δ_η is independent of *both* $\mathbf{k}$ and $\mathbf{k}'$, and depends only on the *energy* of the initial state. This is assumed in nearly all Monte Carlo models, and implies that the strength of the coupling of the electrons to

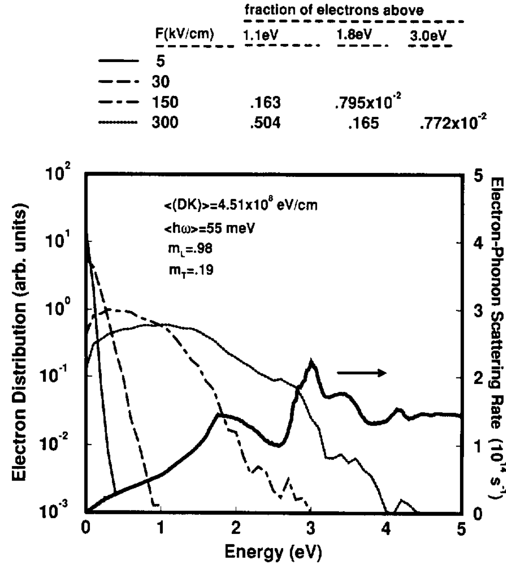

Fig. 20. Full band model [23]; no adjustable electron-phonon parameters in this model. (Kunikiyo, Mizuno, Kamakura, Takenaka, Taniguchi, Hamaguchi).

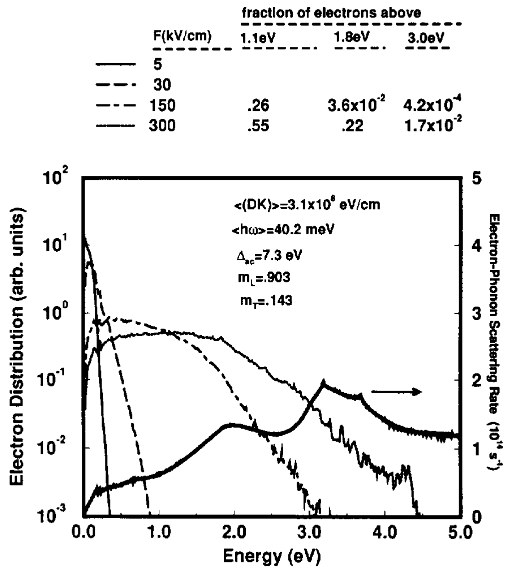

Fig. 21. Full band model [26]; no adjustable eletron-phonon parameters in this model. (Yoder, Hess).

the phonons is constant on equi-energy surfaces. We can then write the scattering rate in the form

$$\frac{1}{\tau(E)} = \frac{2\pi}{\hbar} \sum_{\eta} \left[\frac{\hbar}{2\rho V \omega_{\mathbf{q},\eta}}\right] \Delta_{\eta}^{2} \sum_{\mathbf{k}'} \delta(E(\mathbf{k}') - E \pm \hbar\omega_{\mathbf{q},\eta}) \times (N_{\mathbf{q},\eta} + 1/2 \pm 1/2). \tag{A3}$$

Let us first consider intervalley scattering. This process is frequently referred to as "nonpolar optical" intervalley

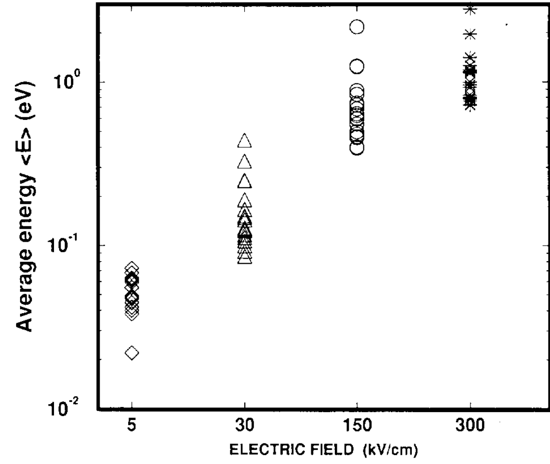

Fig. 22. The average electron energy corresponding to the electron distributions shown in the previous figures.

scattering, although in principle acoustic phonons contribute as well. Indeed this is the model used by nearly all silicon Monte Carlo codes, with the exceptions being those represented in Figs. 19–21. A significant assumption is that the optical phonon dispersion is flat (i.e., ω is independent of $\mathbf{q}$), which allows a simplification of (A3), by removing the $\mathbf{q}$ subscripts:

$$\frac{1}{\tau(E)} = \frac{2\pi}{\hbar} \sum_{\eta} \left[\frac{\hbar}{2\rho V \omega_{\eta}}\right] \Delta_{\eta}^{2}(N_{\eta} + 1/2 \pm 1/2) \times \sum_{\mathbf{k}'} \delta(E(\mathbf{k}') - E \pm \hbar\omega_{\eta}). \tag{A4}$$

We will retain the general notation Δ_η for the coupling strength, although it is common to denote the *intervalley* coupling constant by (DK) for historical reasons dating back to the work of Seitz [33]. The sum over $\mathbf{k}'$ of the energy conserving delta function gives simply the density of final (after scattering) states, so with the approximations made so far the energy dependence of the scattering rate at a given energy is proportional to the density of final states.

At this point we have simplified the scattering rate as far as we can without making critical assumptions about the energy-momentum relation, i.e., the band model. There are a variety of methods by which one can calculate the bandstructure, with varying degrees of accuracy, and these calculations are far beyond the scope of this summary. Given a theory and computational model for calculating $E(\mathbf{k})$ throughout the Brillouin zone (some examples of these theories are given in [32]), one can evaluate the scattering rates based on this bandstructure directly using (A4). A newer class of band models are "fit band models" which are essentially a set of analytic functions which contain free parameters which can be adjusted to agree with, for example, the density of states calculated with a physical model. Again, the details of these models are complicated and it is not appropriate to discuss them here. Near the conduction band minima, however, it is possible to express the bands as simple analytic functions with physically meaningful, and derivable, parameters. These

models allow us to perform the sum over final states ($\mathbf{k}'$) in (A4) analytically, and for clarity this is the route we shall follow below.

A common model is the so-called "nonparabolic model," which can be derived from $\mathbf{k}\cdot\mathbf{p}$ theory of the bandstructure (see [32]). For silicon the equi-energy surfaces near the conduction band minima are ellipsoids of revolution and the theory yields an energy-momentum relation given by

$$E(1+\alpha E) = \frac{\hbar^2}{2}\left(\frac{(k_1-k_{01})^2}{m_t} + \frac{(k_2-k_{02})^2}{m_l} + \frac{(k_3-k_{03})^2}{m_t}\right) \quad \text{(A5)}$$

where we have taken the major axis of the ellipsoid in this case along the k_2 direction (the longitudinal effective mass, m_l is larger than the transverse effective mass m_t), and $\mathbf{k}_0 = (k_{01}, k_{02}, k_{03})$ is the position of the conduction band minimum. Further simplification can be made by setting the parameter α to zero, which gives a parabolic, or free-electron-like energy-momentum relation. If we set $m_l = m_t$ the surfaces of constant energy are spheres. The most simplified band model, "spherical, parabolic bands" then have $E = \frac{\hbar^2|\mathbf{k}|^2}{2m}$. One would use an effective mass for m here, but this is essentially the dispersion relation of a free particle. These last two approximations could be carried through below, but we shall maintain some generality and use (A5) in what follows.

In silicon there are six equivalent minima as described by (A5), ellipsoids oriented along each of the equivalent $\langle 100\rangle$ axes in $\mathbf{k}$ space. With this assumption we can perform the sum over final states analytically, which yields

$$\frac{1}{\tau(E)} = \sum_{\eta,i} \frac{\Delta_{\eta i}^2 m_D^{3/2} Z_i}{\sqrt{2}\pi\rho\hbar^3\omega_\eta}\sqrt{E'(1+\alpha E')}(1+2\alpha E') \times (N_\eta + 1/2 \pm 1/2) \quad \text{(A6)}$$

where $E' = E \mp \hbar\omega_\eta$, i labels a set of equivalent final valleys all oriented similarly with respect to the initial valley, Z_i is the degeneracy of the final valleys, and m_D is the density-of-states effective mass given by $(m_t^2 m_l)^{1/3}$. If we consider the conduction band of silicon with six equivalent minima each with its principal axis oriented along one of the $\langle 100\rangle$ axes, we can categorize the intervalley scattering events into two sets of final valleys. Intervalley scattering to the valley on the opposite side of the Brillouin zone (e.g., $\langle 1,0,0\rangle$ to $\langle -1,0,0\rangle$) is referred to as "g-type" scattering, $Z_g = 1$; scattering to one of the perpendicular valleys (e.g., $\langle 1,0,0\rangle$ to $\langle 0,1,0\rangle$) is "f-type" with $Z_f = 4$. (The notation "f-type" and "g-type" appears to have originated with the work of Morin *et al.* [38] and the labels f and g have no particular significance).

In the case of a multi-band model the total scattering rate $\frac{1}{\tau(E)}$ can be evaluated by averaging over all bands v

$$\sum_v \frac{D_v(E)}{D(E)}\frac{1}{\tau_v(E)} \quad \text{(A7)}$$

where $D(E)$ is the total density of states and $D_v(E)$ is the density of states in band v. $1/\tau_v(E)$ is the rate for out-scattering from band v into all other allowed bands.

The long wavelength acoustic modes present a more difficult problem since we cannot assume that the phonon energy is independent of the wavevector $\mathbf{q}$. Therefore the integration over the energy-conserving delta function, multiplied by the Bose–Einstein factor $N_{\mathbf{q},\eta}$ requires more effort. Different approaches to acoustic phonon scattering can be found in [13], [39], but in general the material properties which control the scattering rate for intravalley acoustic scattering are again the bandstructure, which can be represented by the effective mass(es) as above, and a coupling constant referred to as the acoustic deformation potential. For long wavelength acoustic scattering the first nonvanishing term in powers of q is the linear term, and so the acoustic deformation potential appears in the product $\Delta_{ac}q$, where q is the magnitude of the phonon wave vector. The product appears in place of the constant Δ_η above.

To condense the sometimes complicated scattering models to a few representative numbers we use the "effective intervalley deformation potential"

$$(DK)_{ij} = \left[\sum_\eta \Delta_\eta^2\right]^{\frac{1}{2}} \quad \text{(A8)}$$

and the "effective intervalley phonon energy"

$$(\bar{\hbar\omega})_{ij}^{1} = \frac{1}{(DK)_{ij}^2}\sum_\eta \frac{\Delta_\eta^2}{\hbar\omega_\eta} \quad \text{(A9)}$$

which were introduced in [14]. The subscripts ij indicate a pair of states, e.g., initial and final valleys in the conduction band. The product $(DK)_{ij}^2(\bar{\hbar\omega})_{ij}^{-1}$ is proportional to the strength of the intervalley scattering from valley i to valley j at zero temperature. In the case of the conduction band minima of silicon then, to get the total effective quantities one must average over four f-type processes, and 1 g-type process. For example, for both f- and g-type cases there may be a number of phonon branches η included in a particular model, and averaging over these branches is done first according to (A8) and (A9), and the averaging over f- and g-type processes is performed according to $\langle (DK)\rangle = \left[\frac{4(DK)_f^2+(DK)_g^2}{5}\right]^{\frac{1}{2}}$, where $(DK)_f$ and $(DK)_g$ are calculated from (A8). These constants are listed in the figures for each model as some indication of the strength of the electron-phonon interaction at the conduction band minimum.

REFERENCES

[1] These results were initially shown and discussed by several of the participants and others during the Workshop on Computational Electronics, May 1992, Urbana, IL.

[2] Th. Vogelsang and W. Haensch, "A novel approach for including band structure effects in a Monte Carlo simulation of electron transport in silicon," *J. Appl. Phys.*, vol. 70, pp. 1493–1499, 1991.

[3] J. Y. Tang and K. Hess, "Impact ionization of electrons in silicon," *J. Appl. Phys.*, vol. 54, pp. 5193–5144, 1983.

[4] R. Brunetti, C. Jacoboni, F. Venturi, E. Sangiorgi, and B. Ricco, "A many-band silicon model for hot electron transport at high energies," *Solid-State Electron.*, vol. 32, pp. 1663–1667, 1989.

[5] S. Ramaswamy, "An improved hydrodynamic transport model for silicon extracted from self-consistent Monte Carlo data," M.S. thesis, Univ. Massachusetts, Amherst, MA, 1992.

[6] P. D. Yoder, J. M. Higman, J. Bude and K. Hess, "Monte Carlo simulation of hot electron transport in Si using a unified pseudopotential description of the crystal," *Semicond. Sci. and Technol.*, vol. 7, pp. B357–B359, 1992.

[7] T. Iizuka and M. Fukuma, "Carrier transport simulator for silicon based on carrier distribution Function Evolutions," *Solid-State Electron.*, vol. 33, pp. 27–34, 1990.

[8] C. Jacoboni, R. Minder, and G. Majni, "Effects of band non-parabolicity on electron drift velocity in silicon above room temperature," *J. Phys. Chem. Solids*, vol. 36, pp. 1129–1133, 1975.

[9] R. Thoma, H. J. Peifer, W. L. Engl, W. Quade, R. Brunetti, and C. Jacoboni, "An improved impact-ionization model for high-energy electron transport in Si with Monte Carlo simulation," *J. Appl. Phys.*, vol. 69, pp. 2300–2311, 1991.

[10] H. J. Peifer, B. Meinerzhagen, R. Thoma, and W. L. Engl, "Evaluation of impact ionization modeling in the framework of hydrodynamic equations," *IEDM Tech. Dig.*, pp. 131–134, 1991.

[11] C. Fiegna and E. Sangiorgi, "Modeling of high energy electrons in MOS devices at the microscopic level," *IEEE Trans. Electron Devices*, vol. 40, pp. 619–627, 1993.

[12] C. Fiegna, *et al.*, "Efficient non-local modeling of the electron energy distribution in sub-micron MOSFET's," *IEDM Tech. Dig.*, p. 451, 1990.

[13] M. V. Fischetti and S. Laux, "Monte Carlo analysis of electron transport in small semiconductor devices including band-structure and space-charge effects," *Phys. Rev. B*, vol. 38, pp. 9721–9745, 1988.

[14] M. V. Fischetti, "Monte Carlo simulation of transport in technologically significant semiconductors of the diamond and zinc-blende structures—part 1: homogeneous transport," *IEEE Trans. Electron Devices*, vol. 38, pp. 634–649, 1991.

[15] C. Jacoboni and L. Reggiani, "The Monte Carlo method for the solution of charge transport in semiconductors with application to covalent materials," *Rev. Mod. Phys.*, vol. 55, pp. 645–705, 1983.

[16] A. Phillips, Jr. and P. J. Price, "Monte Carlo calculations on hot electron energy tails," *Appl. Phys. Lett.*, vol. 30, pp. 528–530, 1977.

[17] H. Kosina and S. Selberherr, "Coupling of Monte Carlo and drift diffusion methods with application to metal oxide semiconductor field effect transistors," *Jpn. J. Appl. Phys.*, vol. 29, pp. 2283–2285, 1990.

[18] P. Hesto, "Simulation Monte Carlo du transport non stationnaire dans les dispositifs submicroniques: importance du phenomene balistique dan GaAs a 77 K," These Doctorat es Sciences, Orsay, France, 1984.

[19] M. Mouis, "Etude theorique du fonctionnement des dispositifs a effect de champ haute mobilite a heterojonction," These Doctorat es Sciences, Orsay, 1988.

[20] H. Mizuno, K. Taniguchi, and C. Hamaguchi, "Carrier transport analysis with Monte Carlo simulation including new simplified band structure," *Semicond. Sci. Technol.*, vol. 7, pp. B379–B381, 1992.

[21] N. Sano, M. Tomizawa, and A. Yoshii, "Monte Carlo analysis of hot electron transport and impact ionization in silicon," *Jpn. J. Appl. Phys*, vol. 30, pp. 3662–3665, 1991.

[22] N. Sano and A. Yoshii, "Impact-ionization theory consistent with a realistic band structure of silicon," *Phys. Rev. B*, vol. 45, pp. 4171–4180, 1992.

[23] T. Kunikiyo, T. Kamakura, M. Yamaji, H. Mizuno, M. Takenaka, K. Taniguchi, and C. Hamaguchi, "Adjustable-parameter-free Monte Carlo simulation for electron transport in silicon including full band structure," *Proc. 1993 VPAD* (Int. Workshop on VLSI Process and Device Modeling), p. 40, 1993.

[24] X. Wang, V. Chandramouli, C. M. Maziar, and A. F. Tasch, "Simulation program suitable for hot carrier studies: an efficient multiband Monte Carlo model using both full and analytic bandstructure description for silicon," *J. Appl. Phys.*, vol. 73, pp. 3339–3347, 1993.

[25] S.-L. Wang, N. Goldsman, and K. Hennacy, "Calculation of impact ionization coefficients with a third order Legendre polynomial expansion of the distribution function," *J. Appl. Phys.*, vol. 71, pp. 1815–1822, 1992.

[26] P. D. Yoder, Ph.D. dissertation, Univ. of Illinois, 1993.

[27] C. Hao, J. Zimmermann, M. Charef, R. Fauquembergue, and E. Constant, "Monte Carlo study of two-dimensional electron gas transport in Si-MOS device," *Solid-State Electron.*, vol. 28, pp. 773–740, 1985.

[28] M. Charef, "Etude des phenomenes de transport au voisinage d'une surface ou d'un interface—application au transistor MOS silicon en regime d'inversion," thesis, Universite des Sciences et Technologies de Lille, France, 1983.

[29] A. Abramo, F. Venturi, E. Sangiorgi, J. Higman, and B. Ricco, "A numerical method to compute isotropic band models from anisotropic semiconductor band structures," *IEEE Trans. Computer-Aided Design*, vol. 12, pp. 1327–1335, Sept. 1993.

[30] C.-S. Yao, D. Chen, R. Dutton, F. Venturi, E. Sangiorgi, and A. Abramo, "An efficient impact ionization model for silicon Monte Carlo simulation," *Proc. 1993 VPAD*, (Int. Workshop on VLSI Process and Device Modeling), p. 42, 1993.

[31] E. M. Conwell, *High Field Transport in Semiconductors.* New York: Academic, 1967.

[32] B. K. Ridley, *Quantum Processes in Semiconductors.* New York, Oxford Univ. Press, 1982.

[33] F. Seitz, "On the mobility of electrons in pure nonpolar semiconductors," *Phys. Rev.*, vol. 37, pp. 549–564, 1948.

[34] W. Harrison, "Scattering of electrons of lattice vibrations in nonpolar crystals," *Phys. Rev.*, vol. 104, pp. 1281–1290, 1956.

[35] W. Shockley and J. Bardeen, "Energy bands and mobilities in monatomic semiconductors," *Phys. Rev.*, vol. 77, pp. 407–408, 1950.

[36] *Monte Carlo Device Simulation: Full Band and Beyond*, K. Hess, ed. Boston: Kluwer, 1991.

[37] G. Baym, *Lectures on Quantum Mechanics.* New York: Benjamin, 1969.

[38] F. J. Morin, T. H. Geballe, and C. Herring, "Temperature dependence of the piezoresistance of high purity silicon and germanium," *Phys. Rev.*, vol. 105, pp. 525–539, 1957.

[39] C. Canali, C. Jacoboni, F. Nava, G. Ottaviani, and A. Alberigi-Quaranta, "Electron drift velocity in silicon," *Phys. Rev. B*, vol. 12, pp. 2265–2283, 1975.

[40] Kazutaka Tomizawa, *Numerical Simulation of Submicron Semiconductor Devices.* Boston: Artech House, 1993.

[41] J. Bude, K. Hess, and G. J. Iafrate, "Impact ionization in semiconductors: effects of high electric fields and high scattering rates," *Phys. Rev. B*, vol. 45, no. 19, pp. 10958–10964, 1992.

[42] E. Cartier, M. V. Fischetti, E. A. Eklund, and F. R. McFeely, "Impact ionization in silicon," *Appl. Phys. Lett.*, vol. 62, pp. 3339–3341, 1993.